Tetraphenylporphyrin-cobalt(III) Bis(1,2-dicarbollide) Conjugates: From the Solution Characteristics to Inhibition of HIV Protease

ARTICLE *in* THE JOURNAL OF PHYSICAL CHEMISTRY B · MAY 2007

Impact Factor: 3.3 · DOI: 10.1021/jp066494p · Source: PubMed

9 AUTHORS, INCLUDING:

Pavel Kubát
Academy of Sciences of the Czech Republic
164 PUBLICATIONS **1,935** CITATIONS
SEE PROFILE

Petr Cigler
Academy of Sciences of the Czech Republic
51 PUBLICATIONS **931** CITATIONS
SEE PROFILE

Pavel Matejicek
Charles University in Prague
46 PUBLICATIONS **516** CITATIONS
SEE PROFILE

Vladimir Kral
University of Chemistry and Technology, Pra…
436 PUBLICATIONS **6,685** CITATIONS
SEE PROFILE

Tetraphenylporphyrin-cobalt(III) Bis(1,2-dicarbollide) Conjugates: From the Solution Characteristics to Inhibition of HIV Protease

Pavel Kubát,*,† Kamil Lang,*,‡ Petr Cígler,§,|| Milan Kožíšek,|| Pavel Matějíček,# Pavel Janda,† Zdeněk Zelinger,† Karel Procházka,# and Vladimír Král§,⊥

J. Heyrovský Institute of Physical Chemistry, v.v.i., Academy of Sciences of the Czech Republic, Dolejškova 3, 182 23 Praha 8, Institute of Inorganic Chemistry, v.v.i., Academy of Sciences of the Czech Republic, 250 68 Řež, Department of Analytical Chemistry, Institute of Chemical Technology, Technická 5, 166 28 Praha 6, Institute of Organic Chemistry and Biochemistry, v.v.i., Academy of Sciences of the Czech Republic, Flemingovo nám. 2, 166 10 Praha 6, Department of Physical and Macromolecular Chemistry, Faculty of Science, Charles University in Prague, Hlavova 2030, 128 40 Praha 2, and Zentiva, a.s. Praha, U kabelovny 130, 102 37 Praha 10, Czech Republic

Received: October 3, 2006; In Final Form: February 19, 2007

Tetraphenylporphyrin conjugates with one (**PB1**) and four (**PB4**) cobalt(III) bis(1,2-dicarbollide) substituents were synthesized and the physicochemical and photophysical properties as well as inhibition of HIV-1 protease were described. In methanol, both **PB1** and **PB4** were monomeric producing the triplet states and singlet oxygen after excitation. The triplet states of **PB4** were quickly protonated. Porphyrins exhibited a small decrease of the quantum yields of the singlet oxygen formation (17% for **PB4** and 13% for **PB1**) as compared with 5,10,15,20-tetrakis(4-sulfonatophenyl)porphyrin. On the contrary, no singlet oxygen was detected in aqueous solutions because of strong aggregation. Light scattering and atomic force microscopy (AFM) measurements documented that the behavior of aggregates in aqueous solutions is fairly complex and depends on pH, concentration, and aging. The aggregation started from spherical particles in neutral solutions. In acidic solutions, extended aggregation occurred because of slow protonation of the porphyrin pyrrole nitrogen atoms. Both **PB1** and **PB4** are new representatives of nonpeptide HIV-1 protease inhibitors. Their activity increased with the increasing number of the cobalt(III) bis(1,2-dicarbollide) substituents and was characterized with the IC_{50} values of 290 ± 44 nM for **PB1** and 77 ± 13 nM for **PB4**.

1. Introduction

Porphyrins[1] and boron compounds[2] have been widely investigated as anticancer drugs capable of destroying cancer cells via photodynamic (PDT) and boron neutron capture therapy (BNCT). Therefore, it is a logical effort to combine the porphyrin moiety with boron cluster building blocks to bring together both methods of cancer treatment.[3−10] In this respect, the synthesis of several porphyrins containing carboranyl substituents has been recently reported.[4,5] The amphiphilic conjugates have been mostly associated with low-density lipoproteins (LDL) that can serve as transport vehicles in the blood stream. Tetraphenylporphyrins (structure **I**, Figure 1) with the *nido*-carboranyl substituents, first reported by Haushalter and Rudolph,[6] show enhanced basicity and binding at physiological conditions to negatively charged biopolymers, such as DNA.[7] The cobalt(III) bis(1,2-dicarbollide) substituents (**II**) contain 2 times more boron atoms than *nido*-carboranyls while still bearing a delocalized negative charge. It is anticipated that these conjugates will be promising boron carriers for BNCT.[8,9]

Porphyrins are a typical example of chromophores with a strong tendency to form several types of aggregates.[11] The aggregation depends on the structure and functionalization of porphyrins, ionic strength, temperature, and pH and on the presence of carrier molecules like surfactants.[12,13] Information on the porphyrin self-assembly is important since the aggregation affects the physicochemical properties, pharmacokinetics, interaction with biological membranes, and biological activity of individual molecules.[14] The rational functionalization of the

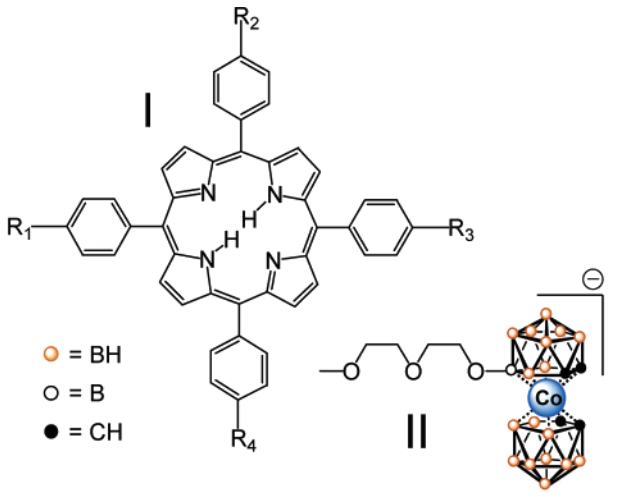

PB4: $R_1=R_2=R_3=R_4=$ **II** **PB1**: $R_1=R_2=R_3=$ H, $R_4=$ **II**

Figure 1. Structures of tetraphenylporphyrin (**I**), cobalt(III) bis(1,2-dicarbollide) substituent (**II**), **PB1**, and **PB4.**

* To whom correspondence should be addressed. E-mail: pavel.kubat@jh-inst.cas.cz; lang@iic.cas.cz.
† J. Heyrovský Institute of Physical Chemistry v.v.i.
‡ Institute of Inorganic Chemistry v.v.i.
§ Institute of Chemical Technology.
|| Institute of Organic Chemistry and Biochemistry v.v.i.
Charles University.
⊥ Zentiva a.s. Praha.

10.1021/jp066494p CCC: $37.00
Published on Web 04/11/2007

porphyrin periphery allows for the preparation of porphyrin conjugates differing in charge, size, and hydrophobicity. The interest in porphyrins bearing polar-lipophilic substituents or substituents with a low polarizability stems from the fact that such substituents can facilitate the transport of porphyrin molecules through biological membranes.[15] By the same token, the lipophilic substituents cause the porphyrin aggregation in aqueous solutions. Introduction of boron atoms offers unique possibilities to tune the physicochemical properties of porphyrins and their ability to penetrate into cancer cells. Here, we present tetraphenylporphyrins with one or four cobalt(III) bis(1,2-dicarbollide) substituents (**PB1** and **PB4**, Figure 1) attached to the porphyrin moiety via flexible polar spacers. Porphyrin **PB4**, first synthesized by Hao and Vicente,[8] combines a good solubility and high pK_a of the protonated *nido*-carboranylporphyrin ring[5] with a large number of the boron atoms in the macrocycle periphery. So far, limited information on photophysical properties of carboranyl-containing porphyrinoid compounds has been published.[16] These results indicate that the presence of carborane clusters do not substantially alter the photosensitizing properties provided that the clusters do not affect protonation of the porphyrin nitrogens and aggregation. In this respect, the cobalt(III) bis(1,2-dicarbollide) clusters are hydrophobic as indicated by the behavior of metallacarboranes forming fairly monodisperse spherical aggregates with radii ca. 100 nm in aqueous solutions.[17] We present the effects of the cobalt(III) bis(1,2-dicarbollide) substituents on the aggregation, protonation, and photophysical properties of the conjugate, namely, the formation of the porphyrin triplet states and singlet oxygen $O_2(^1\Delta_g)$ that is a key cytotoxic species in the photodynamic cancer treatment. Moreover, metallacarboranes were identified as promising pharmacological tectons for nonpeptidic inhibitors of HIV-1 protease.[18] HIV-1 protease represents a prime target for rational drug design, and HIV-1 protease inhibitors are currently used as powerful antiviral drugs. Most of the known protease inhibitors are pseudopeptide compounds with limited bioavailability and stability, and their use is compromised by high costs, side effects, and development of resistant strains. We have also tested **PB4** and **PB1** as potential HIV-1 protease inhibitors.

2. Experimental Section

Materials. The tetrasodium salt of 5,10,15,20-tetrakis(4-sulfonatophenyl)porphyrin (TPPS, Aldrich), tetraphenylporphyrin (TPP, Aldrich), 5,10,15,20-tetrakis(4-hydroxyphenyl)-porphyrin (Porphyrin Systems, Lübeck, Germany), and 8-dioxane-3-cobalt bis(1,2-dicarbollide) (Katchem Ltd., Řež u Prahy, Czech Republic) were used as purchased.

Synthesis of PB1. 5-(4-Hydroxyphenyl)-10,15,20-triphenylporphyrin (50 mg, 0.079 mmol) was added to a suspension of NaH (5.3 mg, 0.22 mmol) in dry 1,2-dimethoxy ethane (1.5 mL) followed by heating to 60 °C for 10 min under argon atmosphere. 8-Dioxane-3-cobalt bis(1,2-dicarbollide) (35.7 mg, 0.087 mmol) was added and the reaction mixture was kept at 70 °C for 2 h. After cooling to ambient temperature, a few drops of a 10% acetic acid aqueous solution were added to destroy the excess NaH, and the solvent was removed in vacuo. The solid phase was suspended in water and was extracted three times by ethyl-acetate. The combined organic phases were reextracted by water, were dried using Na_2SO_4, were filtered, and were evaporated in vacuo. The dry crude product was dissolved in a chloroform/methanol mixture (90:10 v/v), was soaked into a silica gel column, and was eluted with the same solvent mixture. The major green product was collected and evaporated in vacuo yielding 61 mg of the dry sodium salt (72%).

Mass spectra (M.S.) $m/z = 1041$ (100) $[M]^-$ (calcd 1040.57); ^{1}H NMR (acetone-d_6, 300 MHz): 8.82 m (2H, pyrrol), 8.73 m (6H, pyrrol), 8.11−8.14 m (6H, *o*-PheH), 8.01 d (2H, $J = 8.1$ Hz, subst. *m*-PheH), 7.69−7.71 m (9H, subst. *m*,*p*-PheH), 7.27 d (2H, $J = 8.1$ Hz, subst. *o*-PheH), 4.31 t (2H, $J = 4.8$ Hz, $-O-CH_2-CH_2-$), 4.29 br s (2H, $-O-CH_2-CH_2-$), 4.18 br s (2H, $-O-CH_2-CH_2-$), 3.88 t (2H, $J = 4.8$ Hz, $-O-CH_2-CH_2-$), 3.58 s (4H, $CH_{carb.}$), 0.8−3.8 br (17H, BH), −2.86 s (2H, NH). UV/vis (methanol, λ_{max}, nm (ϵ, $M^{-1}cm^{-1}$)): 311 (4.0×10^4), 414 (4.2×10^5), 513 (1.7×10^4), 549 (9.0×10^3), 590 (5.5×10^3), 645 (4.0×10^3). Fluorescence (methanol, λ_{max}, nm): 651 and 718 nm.

Synthesis of PB4. 5,10,15,20-Tetrakis(4-hydroxyphenyl)-porphyrin (50 mg, 0.074 mmol) was added to a suspension of NaH (20 mg, 0.83 mmol) in dry 1,2-dimethoxy ethane (3 mL) followed by heating to 60 °C for 10 min under argon atmosphere. 8-Dioxane-3-cobalt bis(1,2-dicarbollide) (133.2 mg, 0.324 mmol) was added, and the reaction mixture was maintained at 70 °C for 6 h. After cooling to the ambient temperature, a few drops of a 10% acetic acid aqueous solution were added to destroy the excess NaH. The solvent was removed in vacuo. The solid was suspended in water and was extracted three times by ethyl-acetate. The combined organic phases were reextracted by water, were dried using Na_2SO_4, were filtered, and were evaporated in vacuo. The dry crude product was dissolved in a chloroform/methanol mixture (85:15 v/v), was soaked into a silica gel column, and was eluted with the same solvent mixture. Only the major green product was collected and evaporated in vacuo yielding 133 mg of the dry tetrasodium salt (75%). The ^{1}H NMR shifts were assigned using COSY NMR and are equivalent to the published assignment.[8]

M.S. $m/z = 579.6$ (100) $[M]^{4-}$ (calcd 579.51); ^{1}H NMR (acetone-d_6, 300 MHz): 8.92 s (8H, pyrrol), 8.15 d (8H, arom.), 7.40 d (8H, arom.), 4.47 s (8H, $O-CH_2-CH_2-O$), 4.35 s (8H, $O-CH_2-CH_2-O$), 4.31 s (8H, CH_{carb}), 4.01 s (8H, CH_{carb}), 3.75 d (16H, $O-CH_2-CH_2-O$), 1.5−3.1 m (68H, BH), −2.74 s (2H, NH). UV/vis (methanol, λ_{max}, nm (ϵ, $M^{-1}cm^{-1}$)): 313 (1.1×10^5), 418 (4.1×10^5), 516 (1.5×10^4), 554 (1.1×10^4), 592 (5.5×10^3), 649 (5.9×10^3). Fluorescence (methanol, λ_{max}, nm): 659 and 722 nm.

Solutions. The stock solutions of porphyrins (ca. 200 μM) were prepared in methanol (Riedel-de Haën, HPLC grade), were stored in the dark, and were diluted with methanol, redistilled water, or phosphate buffer (20 mM phosphate buffer, pH 7.1) prior to use. The protonation experiments were performed by adding drops of formic acid to methanol solutions. In aqueous solutions, the pH values were adjusted by NaOH or HCl. For light-scattering measurements, all stock solutions were filtered through a 0.20 μm Acrodisc filter before mixing.

NMR and Mass Spectroscopy. ^{1}H and ^{13}C NMR spectroscopy was performed on a Varian Unity-300 instrument and mass spectrometry was performed on a Bruker Esquire 3000 instrument using electrospray ionization. Negative ions were detected.

Absorption and Fluorescence Spectroscopy. The UV/vis absorption spectra were measured on a Perkin-Elmer Lambda 19 or Perkin-Elmer Lambda 35 spectrophotometers. The fluorescence spectra were recorded using a Perkin-Elmer LS 50B luminescence spectrophotometer. All fluorescence emission spectra were corrected for the characteristics of the detection monochromator and photomultiplier as described elsewhere.[19] Resonance light-scattering (RLS) experiments were performed

on a Perkin-Elmer LS 50B luminescence spectrophotometer using simultaneous scans of excitation and emission monochromators through a range of 300−600 nm.

Laser Flash Photolysis. Laser flash photolysis experiments were performed with a Lambda Physik FL 3002 dye laser (λ_{exc} = 414 − 440 nm, output 0.1−5 mJ/pulse) pumped by a Lambda Physik COMPEX 102 excimer (308 nm, fwhm 28 ns). The transient spectra were measured within 300−700 nm using a laser kinetic spectrometer (Applied Photophysics, U.K.) equipped with a 250 W Xe lamp, pulse unit, and R928 photomultiplier (Hamamatsu). Where appropriate, oxygen was removed from a solution by purging with argon.

Luminescence of $O_2(^1\Delta_g)$. Time-resolved near-infrared luminescence at 1270 nm was observed at the right angle to excitation light (Lambda Physik FL 3002 dye laser, λ_{exc} = 418 nm) using a homemade detector unit (interference filter, Ge diode Judson J16-8SP-R05M-HS). The quantum yields of singlet oxygen Φ_Δ were estimated by the comparative method using TPPS as a standard.[20] Incident energy used is within the energy region where the intensity of a luminescence signal is directly proportional to the incident energy (less than 500 μJ).

Atomic Force Microscopy (AFM). The porphyrin nanostructures were imaged using a tapping mode AFM (Nanoscope IIIa, Veeco, U.S.). The nanostructures were prepared by casting a droplet (20−50 μL) of a porphyrin solution onto a mica substrate. The droplet was removed after a certain time and mica was dried in ambient air.

Dynamic Light Scattering (DLS). The light-scattering setup (ALV, Langen, Germany) consisted of a 633 nm He−Ne laser, an ALV CGS/8F goniometer, an ALV High QE APD detector, and an ALV 5000/EPP multibit, multitau autocorrelator. The measurements were carried out for different angles (from 30 to 150 degrees) at 20 °C. The data analysis was performed by fitting the measured normalized autocorrelation function $g_2(t) = 1 + \beta|g_1(t)|$,[2] where $g_1(t)$ is the electrical field correlation function, t is the lag time, and β is a factor accounting for deviation from the ideal correlation. An inverse Laplace transform of $g_1(t)$ with the aid of a constrained regularization algorithm (CONTIN) provides the distribution of relaxation times, $\tau A(\tau)$

$$g_1(t) = \int \tau A(\tau)\exp(-t/\tau)\mathrm{d}\ln\tau \qquad (1)$$

Effective diffusion coefficients were calculated from individual diffusion modes as $D^{eff} = \Gamma/q^2$, where $\Gamma = 1/\tau$ and $q = (4\pi n_0/\lambda)\sin(\theta/2)$ is the magnitude of the scattering vector. Here, θ is the scattering angle, n_0 is the refractive index of pure solvent, and λ is the wavelength of the incident light. Hydrodynamic radii, R_H, were evaluated from the true diffusion coefficients, D, using the Stokes−Einstein formula, $R_H = kT/(6\pi D\eta)$, where D was obtained by the extrapolation of D^{eff} to the zero scattering angle.

Static Light Scattering (SLS). The measurements were performed on the same instrument as DLS. The data were treated by the standard Zimm method: the values of $Kc/R^{cor}(q, c)$ were measured, where $K = (4\pi^2 n^2(\mathrm{d}n/\mathrm{d}c)^2)/(\lambda^4 N_A)$ is a constant containing the refractive index, n, of the solvent, the refractive index increment of colloidal particles with respect to the solvent, $(\mathrm{d}n/\mathrm{d}c)$, the wavelength of the incident light, λ, and the Avogadro constant, N_A, and $R^{cor}(q, c)$ is the corrected Rayleigh ratio, which depends on the sample concentration c and on the scattering vector q.

Since the refractive index increment $(\mathrm{d}n/\mathrm{d}c)$ and actual concentration of scattering particles are unknown, the SLS data were used only to obtain the form factor, $P(q)$, by dividing extrapolated values of $Kc/R(c)$ to the zero angle by the apparent values of $Kc/R(q, c)$, where c is the concentration of porphyrin and the $(\mathrm{d}n/\mathrm{d}c)$ value is arbitrary. The radius of gyration, R_g, was calculated according to the relationship $P^{-1}(q) = 1 + (1/3)R_g^2q^2$.

The Preparation and Inhibition of Wild-Type HIV-1 Protease. Protease expression, refolding, and purification were performed as described in the literature.[21] Briefly, HIV-1 protease encoded in the expression plasmid was expressed as inclusion bodies in *Escherichia coli* BL21 (DE3). The inclusion bodies were then washed with three different buffers and were solubilized in 8 M urea. Protease was refolded by dialysis and was purified by batch chromatography on QAE Sephadex and cation exchange fast protein liquid chromatography using a MonoS column.

The IC_{50} value was determined by the spectrophotometric assay with the chromogenic substrate KARVNleNphEANle-NH_2 on the basis of the absorbance decrease at 305 nm because of the substrate cleavage.[21] Typically, 9 pmol of protease was added to 1 mL 0.1 M sodium acetate buffer, pH 4.7, 0.3 M NaCl, containing the substrate in concentration ranging about the value of K_m of wild-type HIV-1 protease. The tested inhibitor was dissolved in DMSO (its final concentration was less than 2.5%). Protease was incubated in buffer together with the inhibitor for 1 min, and the reaction was initiated by the addition of the substrate. The IC_{50} value was determined from the plot of the ratio of the initial rate of the inhibited and uninhibited reaction versus concentration of the inhibitor using a nonlinear fitting procedure (program Grafit 5.0, Erithacus Software Ltd.). The IC_{50} value expresses the concentration of the inhibitor required for reducing the enzyme activity by 50%. The mechanism of inhibition was derived from the measurement of initial reaction rates versus substrate concentrations in the presence of various concentrations of the inhibitor and was visualized using the double-reciprocal Lineweaver−Burk plot.

3. Results and Discussion

Synthesis. The structures of monosubstituted **PB1** and tetrasubstituted **PB4** studied herein are shown in Figure 1. Porphyrins **PB1** and **PB4** were obtained by reacting appropriate 4-hydroxyphenylporphyrin with 8-dioxane-3-cobalt bis(1,2-dicarbollide)[22] as described by Hao and co-workers.[8,9] We modified the procedure for activation of the porphyrin hydroxyl groups using a stronger base, NaH, instead of sodium or potassium carbonate. In addition, the solvent 1,2-dimethoxyethane was substituted for acetone. These conditions led to significantly reduced reaction times with only a small extent of expensive 8-dioxane-3-cobalt bis(1,2-dicarbollide) giving the yield slightly lower than that of Hao and Vicente.[8] The purification procedure of **PB4** deserves a note. A porphyrin byproduct having the Soret band at 423 nm, the Q-band at 457 nm, and the fluorescence band at 609 nm all in methanol is eluted along with **PB4** when using an acetonitrile−chloroform mixture for separation. A good separation was achieved using a methanol−chloroform mixture.

Spectroscopic Characterization. The UV/vis absorption spectra were measured in methanol where **PB1** (Figure 2a) and **PB4** (Figure 3a) have characteristic absorption bands of monomeric porphyrins: the Soret band and four Q bands. The Lambert−Beer plots show excellent linearity in the range of concentrations investigated (up to 20 μM) indicating no evidence for aggregation in the ground state. The most intensive Soret band is shifted from 414 (**PB1**) to 418 nm (**PB4**) because of an increased number of electron-donating oxygen atoms while the

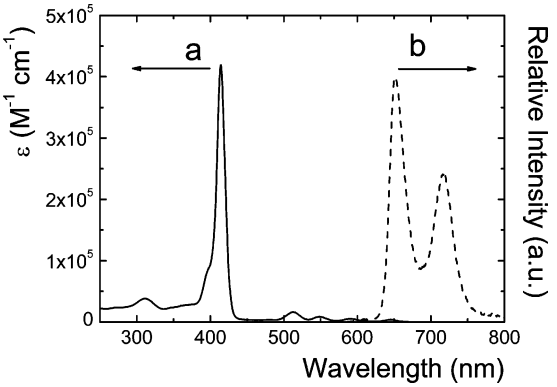

Figure 2. Absorption (a, left axis) and corrected fluorescence emission (b, right axis, dashed line) spectra of **PB1** in methanol. Excited at 414 nm.

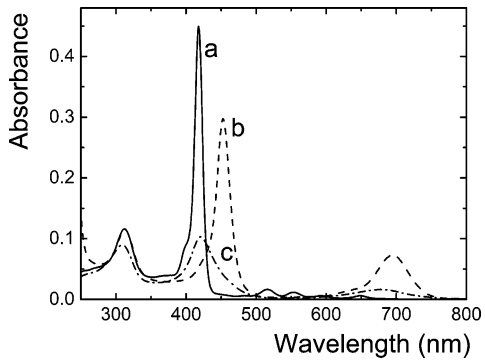

Figure 3. Absorption spectra of 1.1 μM **PB4** in methanol (a), in methanol after acidification by adding formic acid, 0.3% v/v (b, dashed line), and in 20 mM phosphate buffer, pH 7.1 (c, dash-dotted line).

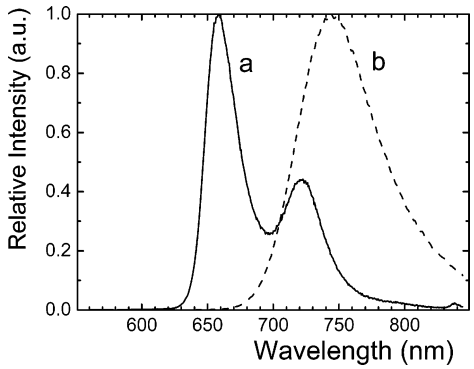

Figure 4. Corrected fluorescence emission spectra of 1.1 μM **PB4** in methanol excited at 418 nm (a) and after acidification (0.3% v/v formic acid) excited at 453 nm (b, dashed line). The spectra are normalized.

molar absorption coefficients remain constant (4.1×10^5 M^{-1} cm^{-1}). The attachment of the cobalt(III) bis(1,2-dicarbollide) substituents does not influence the electronic transitions from the ground state since the resulting absorption spectra are identical to those of corresponding starting hydroxyphenylporphyrins, and it is only indicated by a new absorption band located at 311−313 nm belonging to the absorption of the substituent itself. The fluorescence emission spectra are typical for porphyrins. The bands are at 651 and 718 nm for **PB1** (Figure 2b) and at 659 and 722 nm for **PB4** (Figure 4a). There is no energy transfer from the cobalt(III) bis(1,2-dicarbollide) substituents to the porphyrin moiety when the conjugates are excited at the absorption band of 311−313 nm.

Acidification of **PB4** in methanol leads to a decrease of the absorption at 418 nm and a concomitant appearance of the Soret band at 453 nm and of two Q bands at 633 and 695 nm (Figure 3b). It suggests a double protonation of the pyrrole core increasing the symmetry of the porphyrin moiety. The formation of the zwitterionic molecule is also evidenced by the only fluorescence emission band at 744 nm (Figure 4b). Similarly, the diacid of **PB1** has the absorption bands at 440, 611, and 662 nm and the fluorescence emission band at 700 nm (data not shown).

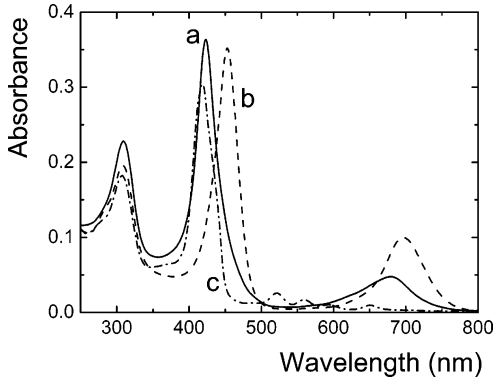

Figure 5. UV/vis spectral changes of ca. 4 μM **PB4** in water (a) following the addition of HCl to pH 1.8 (b, dashed line) and the addition of NaOH to pH 13.0 (dash-dotted line).

The Soret band of **PB4** in phosphate buffer (20 mM, pH 7.1) is red-shifted by 3 nm to 421 nm, considerably broadened with a large hypochromicity effect when compared with methanol solutions. In addition, the Q bands in the region 500−600 nm disappear (Figure 3c). The spectral changes are accompanied by the loss of fluorescence emission. All the changes can be explained by significant porphyrin aggregation as it is documented by SLS and DLS measurements (see below). Cobalt(III) bis(1,2-dicarbollide)(1−) itself is rather hydrophobic and forms spherical aggregates in aqueous solutions.[17] Hence, the aggregation of **PB4** is induced by the attached hydrophobic substituents because the delocalized negative charge on the sandwich polyhedral subclusters is not sufficient to prevent electrostatic repulsion between individual porphyrin molecules. The significance of electrostatic forces for the stabilization of aggregated structures is documented by the fact that the aggregation is considerably accelerated by the addition of electrolyte (like NaCl). The aggregation is evidently controlled by kinetic factors because its extent depends strongly on the incubation time, stirring a solution, and temperature. The Soret band of fresh solutions at 421 nm shifts slowly to higher wavelengths during 24 h standing at room temperature. It indicates a slow structural reorganization of aggregated forms. The corresponding resonance light-scattering (RLS) profiles are similar to those of the pure solvent. The only difference is the intensity minimum around 420 nm because of the porphyrin absorption. The RLS technique allows for the identification of extended aggregated species even at low concentrations as aggregates with observable RLS contain tens of thousands of electronically interacting monomer units at least; oligomers and small aggregates do not show the resonance light scattering.[23] The lack of the RLS signals suggests that electronic interactions between the porphyrin moieties are very weak because they are screened by the bulky peripheral substituents.

Figure 5 compares the visible absorption bands of **PB4** in water (pH 5.9), acid (pH 1.8), and basic solutions. The comparison documents clearly that **PB4** aggregates in pure water. Acidification causes a red shift of the Soret band to 453 nm and the reduction of the number of the Q-bands from 4 to 2 (Figure 5b). No enhancement of the resonance light scattering is observed similarly to the behavior in phosphate buffer. A

TABLE 1: Characterization of PB4 Aggregates by Light Scattering; 1.6 μM PB4

solution	pH	aging/hours	R_H/nm[a]	R_g/nm[b]	R_g/R_H
HCl in water	1.4	0.5	613 ± 33	280 ± 11	0.46
		72[c]	3100 ± 900[c]		
deionized water	5.8	0.5	278 ± 8	288 ± 20	1.04
		72	294 ± 13	346 ± 28	1.18
		170	258 ± 10	271 ± 24	1.05
NaCl in water	5.0	0.5	269 ± 2	280 ± 17	1.04
		72	250 ± 5	247 ± 7	1.00
		170	284 ± 10	293 ± 23	1.03
NaOH in water	10.9	0.5	280 ± 16	243 ± 3	0.87
		72	275 ± 11	226 ± 34	0.82
		170	281 ± 10	193 ± 5	0.70
NaOH in methanol		0.5	252 ± 8	185 ± 22	0.73

[a] DLS. [b] SLS. [c] Slowly precipitates; R_H of particles remaining in a solution exceeds several μm.

new low-intensity fluorescence emission band appears at about 765 nm. The spectral changes can be attributed to the conversion of aggregates (Figure 5a) to their corresponding protonated form. A small contribution of the protonated monomeric species cannot be excluded because of low fluorescence intensity around 765 nm. After adding NaOH to a solution of pH 1.8, the Soret band shifts to 419 nm and four Q-bands at 521, 559, 593, and 650 reappear (Figure 5c). The four Q-bands and the new fluorescence emission bands at 659 and 722 nm indicate deprotonation of aggregates followed by their partial monomerization.

Porphyrin **PB1** behaves similarly to **PB4**. The aggregation in pure water is indicated by the shift of the Soret band to 409 nm and disappearance of the fluorescence emission bands.

Light-Scattering Structural Characterization. The solutions of **PB4** were studied by dynamic (DLS) and static light scattering (SLS). The fact that measured solutions absorb and emit visible light can complicate the light-scattering studies. Fortunately, the absorption of laser light of 633 nm by **PB4** aggregates is negligible and no signs of any absorption or fluorescence effects on the scattered light intensity, such as oscillations of the autocorrelation function[24] or the U-shape of SLS function,[25] were observed.

The light-scattering measurements reveal a significant fraction of multimolecular **PB4** aggregates in aqueous solutions. The aggregation behavior is rather complex and depends strongly on pH. The distributions of correlation times from the DLS measurements always contain one fairly narrow mode. In spite of obvious kinetic effects, it suggests that the aggregation is thermodynamically controlled. The values of the hydrodynamic radius, R_H, radius of gyration, R_g, and the ratio R_g/R_H for solutions differing in the composition and aging time are listed in Table 1.

In acidic solutions, **PB4** forms large and relatively monodisperse aggregates shortly after mixing. The aggregates start to precipitate in several days. The ratio R_g/R_H equals ca. 0.46 at early stages. This is a significantly lower value than that for the hard sphere being 0.775.[26] It indicates that the aggregates are relatively loose and might resemble a structure of microgels[27] as a result of interaction between the negatively charged cobalt(III) bis(1,2-dicarbollide) substituents and the protonated porphyrin moiety. The situation that the corresponding relaxation mode is very narrow and diffusion-controlled indicates that the slow and kinetically controlled precipitation starts from fairly monodisperse and thermodynamically controlled precursors. In neutral or basic solutions, **PB4** forms smaller aggregates characterized by R_g/R_H in the range from 0.7 to 1.2. Because the aggregates are obviously polydisperse and change slightly in time, we cannot retrieve exact information on their shape from the ratio R_g/R_H. We can summarize that compact aggregates of **PB4** have R_g of 250−300 nm and that the size does not dramatically change with time and practically does not depend on pH above 5 and ionic strength.

Porphyrin **PB4** dissolved in methanol behaves differently in respect to aqueous solutions. Methanol solutions even after acidification do not exhibit measurable DLS signals. These results confirm the presence of porphyrin monomers as follows from the UV/vis spectroscopy. In contrast, roughly spherical particles are observed shortly after the addition of NaOH to methanol. The particles disappear in several days.

Porphyrin Nanostructures. Porphyrin aggregates were visualized by atomic force microscopy (AFM) on mica substrates (Figure 6). Although the shape of aggregates can be deformed after their deposition on the substrate and large clusters may split into smaller fragments because of deformation forces acting on the substrate surface, a critical evaluation of AFM images yields valuable information on the shape, polydispersity, and structure of deposited objects.

The AFM images show that the porphyrin nanostructures are fairly complex and depend on concentration, pH, and aging of starting solutions. The predominant structure of **PB4** particles deposited from redistilled water is a compact sphere of a broad size distribution. The mean diameter measured 1 h after deposition is 17 ± 7 nm and the corresponding height is 0.6 ± 0.4 nm (Figure 6a). The spherical shape is in accordance with that of cobalt(III) bis(1,2-dicarbollide)(1−) aggregates studied in the earlier work.[17] After 50 h aging, the particles develop into larger structures, however, still the original spherical particles are present (Figure 6b). In acidic solutions, mostly large aggregates with a complex structure are observed (Figure 6c). Even though we cannot preclude some structural changes caused by deposition, the results are in agreement with the DLS and SLS data (see above).

Triplet States. To explore the effect of the substituets on the triplet-state dynamics of the porphyrin moieties, we carried out transient absorption measurements in methanol and aqueous solutions. Figure 7a shows the transient difference absorption spectrum of fresh **PB1** after excitation in methanol. Similar results were obtained for **PB4**, however, an additional red-shifted band appears at 490−500 nm (Figure 7b). In general, all measured spectra show the typical features of the porphyrin triplet states in solution, that is, a broad positive absorption band within the ∼440−520 nm range arising from triplet−triplet absorption, which is partially depleted by the ground-state absorption associated to the Soret band. Figure 7d and e depicts the time course of the transient absorption of **PB4** in argon-saturated solution at 450 and 500 nm. Clearly, the kinetics of the transients differ indicating that the 500 nm population is formed within the first microsecond after excitation while the triplet states recorded at 450 nm decay monoexponentially in the microsecond time scale (Table 2). Since the 500 nm band is identical to that observed after acidification of **PB4** in methanol (Figure 7c), we attribute the band to the triplet states of the protonated porphyrin moiety. In comparison, analogous experiments with TPPS give only the pure triplet−triplet spectra. These differences can be explained by increased basicity of the porphyrin moiety in porphyrin−boron conjugates[7] and by the fact that the porphyrin is a stronger base in the triplet state than in the ground state.[28,29] The origin of protons could be related to the properties of cobalt bis(1,2-dicarbollide)(1−) anions.[30] The anions cannot accommodate protons and the corresponding very strong acid exists only in the form of the cobalt bis(1,2-

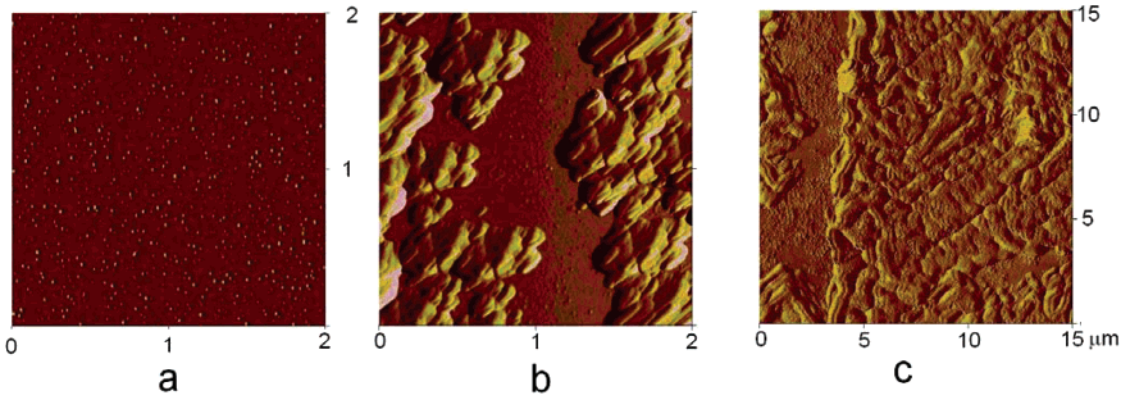

Figure 6. AFM tapping mode image of nanostructures formed by drop casting of an aqueous solution of 8.5 μM **PB4** at pH 6.3: measured 1 (a) and 50 (b) hours after mixing; at pH 2.0: measured 50 h (c) after mixing.

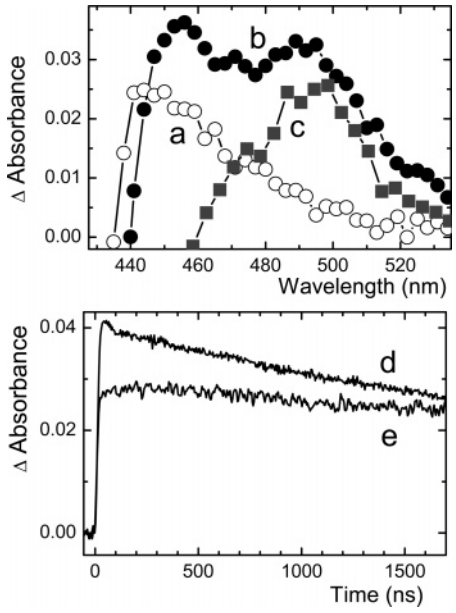

Figure 7. Transient absorption spectra of **PB1** (a) and **PB4** (b) (λ_{exc} = 420 nm) and of **PB4** diacid (c) prepared by adding formic acid (0.3% v/v) (λ_{exc} = 430 nm). The spectra were collected 350 ns after excitation in air-saturated methanol. Decays of the transients of **PB4** were recorded at 450 (d) and 500 (e) nm in argon-saturated methanol.

TABLE 2: Characterization of the PB1 and PB4 Triplet States (λ_{max} Is the Band Maximum; τ_{Ar} Is the Lifetime of the Triplet States) and the Quantum Yields of the $O_2(^1\Delta_g)$ Formation, Φ_Δ, in Air-Saturated Methanol

species	λ_{max} (nm)	τ_{Ar} (μs)	species	λ_{max} (nm)	τ_{Ar} (μs)	Φ_Δ
PB4	450[a]	11[a]	**PB4** diacid	500[b]	6.8[b]	0.57
PB1	450[a]	27[a]	**PB1** diacid	500[b]	14[b]	0.60
TPPS	440[a]	160[a]	TPPS diacid			0.69

[a] In argon-saturated methanol. [b] In argon-saturated methanol; both **PB1** and **PB4** are converted to the diprotonated form by acidification with formic acid (0.3% v/v) (see Figure 3b).

dicarbollide)(1−)/LH^+ pairs where the solvent molecules LH act as a base. In the presence of other molecules in solution, protons are bound to the most basic molecules. In the case of studied porphyrins, fast protonation occurs since pyrrole nitrogen atoms of the porphyrin moiety in the triplet states are the most basic site in the system.

The characteristics of the triplet states are summarized in Table 2. The lifetime of the triplet states, τ_{Ar}, decreases with increasing number of the cobalt(III) bis(1,2-dicarbollide) substituents. The decay of the triplet states is also accelerated in the presence of oxygen and after protonation to porphyrin diacids

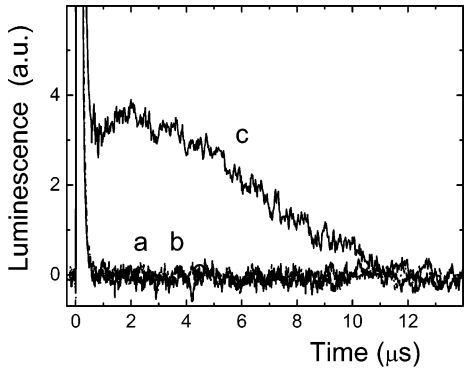

Figure 8. Time dependence of the $O_2(^1\Delta_g)$ luminescence signal at 1270 nm of **PB4** (a), **PB1** (b), and TPPS (c) in air-saturated 20 mM phosphate buffer, pH 7.1. Optically matched solutions at the excitation wavelength (A_{418nm} = 0.286 ± 0.008) were hit by the laser pulse (352 ± 21 μJ). The signals are the average of 1000 traces.

in the ground state. In phosphate buffer, no triplet state signals of **PB1** and **PB4** were found because of strong aggregation.

Singlet Oxygen. The production of $O_2(^1\Delta_g)$ by **PB1** and **PB4** in methanol can be expected on the basis of the transient absorption measurements and observation that title porphyrins are monomeric. To assess the efficiency of $O_2(^1\Delta_g)$ generation, we measured its photoluminescence at λ_{em} = 1270 nm upon pulsed laser excitation. The measured luminescence signals reflect both the duration of the triplet states and the $O_2(^1\Delta_g)$ lifetime. Comparison of the measured $^1O_2$ lifetimes with the lifetime in pure methanol (9−12 μs)[31] confirms that the kinetics of the $O_2(^1\Delta_g)$ disappearance is controlled by solvent effects with no indication of singlet oxygen quenching by porphyrins themselves. The intensities of the $O_2(^1\Delta_g)$ luminescence signals extrapolated to t = 0 generated by optically matched solutions (A_{exc} = 0.250 ± 0.007) were compared to that of TPPS to obtain quantum yields of the $O_2(^1\Delta_g)$ formation, Φ_Δ (Table 2). The Φ_Δ values of **PB1** and **PB4** are comparable with Φ_Δ of TPPS (Φ_Δ = 0.69 in methanol).[20] This allows us to conclude that the cobalt(III) bis(1,2-dicarbollide) substituents on the porphyrin periphery have the minimal effect on the efficiency of the $O_2(^1\Delta_g)$ production.

The aggregation of porphyrins in aqueous solutions leads to a considerable decrease of Φ_Δ because of fast competitive nonradiative transitions within different excited states of the molecule.[32] A typical luminescence trace of $O_2(^1\Delta_g)$, presented in Figure 8c for TPPS, shows the contribution of porphyrin fluorescence and scattered excitation light at the early beginning of the signal (0−500 ns) and the fast decay of $O_2(^1\Delta_g)$ because of its short lifetime in water (τ = 3−4 μs).[31] The luminescence

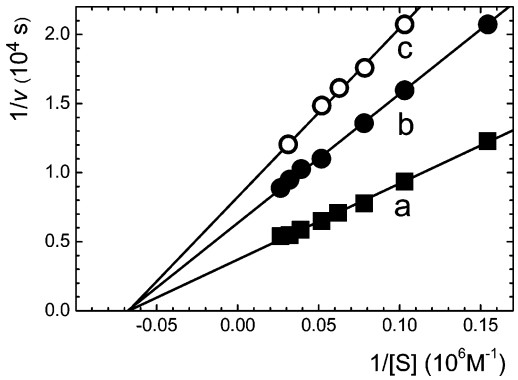

Figure 9. Double-reciprocal plot of the initial reaction rate vs substrate (KARVNleNphEANle-NH_2) concentration at fixed concentrations of **PB4**: 0 nM (a); 60 nM (b); and 80 nM (c).

traces measured for **PB4** and **PB1** in buffer show only the former process, which does not depend on oxygen concentration (Figure 8a, b). These results confirm that aggregated porphyrins do not produce measurable concentrations of $O_2(^1\Delta_g)$. The described strong aggregation preventing the formation of $O_2(^1\Delta_g)$ can be responsible for non-phototoxicity of most porphyrin-cobalt(III) bis(1,2-dicarbollide) conjugates reported recently by Sibrian-Vazquez et al.[10]

Inhibition of HIV-1 Protease. Most of the HIV protease inhibitors currently used in clinics are pseudopeptides or peptide mimetics with a limited number of structural building blocks. Very recently, 12-vertex metallacarborane clusters have been identified as promising, selective, and potent inhibitors of HIV protease.[18] Metallacarboranes represent hydrophobic, stable, nontoxic, and synthetically available moieties that can serve as specific structural analogues of aromatic compounds. Combination of suitable hydrophobicity and delocalized negative charge enables the unique interactions between proteins and the surface of the cluster.

Porphyrins **PB4** and **PB1** were tested as inhibitors of HIV-1 protease in vitro. It was found that the IC_{50} values are 77 ± 13 nM and 290 ± 44 nm for **PB4** and **PB1**, respectively. Four times larger activity of **PB4** bearing four cobalt(III)bis(1,2-dicarbollide) substituents when compared with **PB1** shows that the presence of these substituents is crucial for inhibition of HIV-1 protease. The IC_{50} values are well comparable with those of structurally similar porphyrin inhibitors substituted with dicarba-*closo*-dodecaboranes.[33] The mechanism of inhibition can be derived from the measurement of initial reaction rates versus substrate concentrations in the presence of various concentrations of porphyrin inhibitors followed by casting the data into the double-reciprocal Lineweaver−Burk plots (Figure 9). As indicated by the unaltered Michaelis constant K_M, both **PB4** and **PB1** are noncompetitive inhibitors of HIV-1 protease, that is, both porphyrins have significant binding affinity toward free enzyme and enzyme−substrate binary complex.

The known metallacarborane inhibitors of HIV-1 protease are acting competitively.[18] The different inhibition mechanisms of **PB1** and **PB4** can originate from enhanced hydrophobicity, sterical hindrance, and affinity toward binding sites distinct from the active sites. Nonetheless, even though the interaction with enzyme is noncompetitive, the low IC_{50} values indicate a strong inhibition and high specificity. Porphyrins **PB1** and **PB4** represent the first noncompetitive HIV protease inhibitors containing either metallacarborane or the porphyrin skeleton, widening thus so far a rather limited group of the noncompetitive HIV protease inhibitors.[34−38]

Acknowledgment. The authors thank Dr. Jan Konvalinka (Institute of Organic Chemistry and Biochemistry v.v.i., Academy of Sciences of the Czech Republic, Praha) for critical reading of the manuscript. This research was supported by the Czech Science Foundation (Grant Nos. 203/04/0426, 203/07/1424, and 203/04/0490), the Academy of Sciences of the Czech Republic (Grant No. KAN100500652), the Ministry of Education of the Czech Republic within the Program 1M0508 "Research Centre for new Antivirals and Antineoplastics", and the long-term research plan MSM 0021620857.

References and Notes

(1) Patrice T. *Photodynamic Therapy;* Royal Society of Chemistry: London, 2004.

(2) Barth, R. F.; Coderre, J. A.; Vicente, M. G. H.; Blue, T. E. *Clin. Cancer Res*. **2005**, *11*, 3987−4002.

(3) Miura, M.; Micca, P. L.; Fisher, C. D.; Heinrichs, J. C.; Donaldson, J. A.; Finkel, G. C. *Int. J. Cancer* **1996**, *68*, 114−119.

(4) Vicente, M. G. H.; Shetty, S. J.; Wickramasinghe, A.; Smith, K. M. *Tetrahedron Lett.* **2000**, *41*, 7623−7627.

(5) Clarc, J. C.; Fronzek, F. R.; Vicente, M. G. H. *Tetrahedron Lett.* **2005**, *46*, 2365−2368.

(6) Haushalter, R. C.; Rudolph, R. W. *J. Am. Chem. Soc.* **1978**, *100*, 4628−4629.

(7) Lauceri, R.; Purrello, R.; Shetty, S. J.; Vicente, M. G. H. *J. Am. Chem. Soc*. **2001**, *123*, 5835−5836.

(8) Hao E.; Vicente, M. G. H. *Chem. Commun.* **2005**, 1306−1308.

(9) Hao, E.; Jensen, T. J.; Courtney, B. H.; Vicente, M. G. H. *Bioconjugate Chem.* **2005**, *16*, 1495−1502.

(10) Sibrian-Vazquez, M.; Hao, E.; Jensen, T. J.; Vicente, M. G. H. *Bioconjugate Chem.* **2006**, *17*, 928−934.

(11) Ribó, J. M.; Bofill, J. M.; Crusats, J.; Rubires, R. *Chem.−Eur. J.* **2001**, *7*, 2733−2737.

(12) (a) Maiti, N.; Mazumdar, S.; Periasamy, N. *J. Phys. Chem. B* **1998**, *102*, 1528−1538. (b) Kano, K.; Fukuda, K.; Wakami, H.; Nishiyabu, R.; Pasternack, R. F. *J. Am. Chem. Soc.* **2000**, *122*, 7494−7502.

(13) (a) Kubát, P.; Lang, K.; Procházková, K.; Anzenbacher, P. *Langmuir* **2003**, *19*, 422−428. (b) Kubát, P.; Lang, K.; Anzenbacher, P. *J. Phys. Chem. B* **2002**, *106*, 6784−6792.

(14) Lang, K.; Mosinger, J.; Wagnerová, D. M. *Coord. Chem. Rev.* **2004**, *248*, 321−350.

(15) Maziere, J. C.; Santus, R.; Morliere, P.; Reyftmann, J. P.; Candide, C.; Mora, L.; Salmon, S.; Maziere, C.; Gatt, S.; Dubertret, L. *J. Photochem. Photobiol. B* **1990**, *6*, 61−68.

(16) (a) Spizzirri, P. G.; Hill, J. S.; Kahl, S. B.; Ghiggino, K. P. *Photochem. Photobiol.* **1996**, *64*, 975−983. (b) Vicente, M. G. H.; Gottumukkala, V.; Wickramasinghe, A.; Anikovsky, M.; Rodgers, M. A. J. *Proc. SPIE - The International Society for Optical Engineering* **2004**, 5315 (Optical Methods for Tumor Treatment and Detection: Mechanisms and Techniques in Photodynamic Therapy XIII), 33−40. (c) Friso, E.; Roncucci, G.; Dei, D.; Soncin, M.; Fabris, C.; Chiti, G.; Colautti, P.; Esposito, J.; De Nardo, L.; Rossi, C. R.; Nitti, D.; Giuntini, F.; Borsetto, L.; Jori, G. *Photochem. Photobiol. Sci.* **2006**, *5*, 39−50.

(17) Matějíček, P.; Cígler, P.; Procházka, K; Král, V. *Langmuir* **2006**, *22*, 575−581.

(18) Cígler, P.; Kožíšek, M.; Řezáčová, P.; Brynda, J.; Otwinowski, Z.; Pokorná, J.; Plešek, J.; Grüner, B.; Dolečková-Marešová, L.; Máša, M.; Sedláček, J.; Bodem, J.; Krausslich, H.; Král, V.; Konvalinka, J. *PNAS* **2005**, *102*, 15394−15399.

(19) Gardecki, J. A.; Maroncelli, M. *Appl. Spectrosc.* **1998**, *52*, 1179−1189.

(20) Tanielian C.; Wolff, C. *J. Phys. Chem.* **1995**, *99*, 9825−9830.

(21) Weber, J.; Mesters, J. R.; Lepsik, M.; Prejdova, J.; Švec, M.; Sponarova, J.; Mlcochova, P.; Skalicka, K.; Strisovsky, K.; Uhlikova, T.; Soucek, M.; Machala, L.; Stankova, M.; Vondrasek, J.; Klimkait, T.; Kraeusslich, H. G.; Hilgenfeld, R.; Konvalinka, J. *J. Mol. Biol.* **2002**, *324*, 739−754.

(22) Plešek, J.; Heřmánek, S.; Franken, A.; Císařová, I.; Nachtigal, C. *Collect Czech. Chem. Commun.* **1997**, *62*, 47−56.

(23) (a) Pasternack, R. F.; Collings, P. J. *Science* **1995**, *369*, 935−939. (b) de Paula, C. C.; Robblee, J. H.; Pasternack, R. F. *Biophys. J.* **1995**, *68*, 335−341.

(24) Sehgal, A.; Seery, T. A. P. *Macromolecules* **1999**, *32*, 7807−7814.

(25) Kratochvíl, P. In *Classical Light Scattering from Polymer Solutions, Polymer Science Library 5*; Jennkins, A. D., Ed.; Elsevier: Amsterdam, 1987; p 106.

(26) Burchard, W. *Adv. Polym. Sci.* **1983**, *48*, 1−124.

(27) Burchard, W. In *Light Scattering. Developments and Principles*; Brown, W., Ed.; Clarendon Press: Oxford, U.K., 1996; p 439.

(28) (a) Tsukahara, S.; Watarai, H. *Phys. Chem. Chem. Phys.* **2002**, *4*, 1592−1597. (b) Kubát, P.; Lang, K.; Mosinger, J.; Wagnerová, D. M. *Z. Phys. Chem.* **1999**, *210*, 243−256.

(29) (a) Gensch, T.; Viappiani, C.; Braslavsky, S. E. *J. Am. Chem. Soc.* **1999**, *121*, 10573−10582. (b) Gonçalves, P. J.; De Boni, L.; Barbosa, N.; Neto, M.; Rodrigues, J. J., Jr.; Zílio, S. C.; Borissevitch, I. E. *Chem. Phys. Lett.* **2005**, *407*, 236−241.

(30) Plešek, J.; Baše, K.; Mareš, F.; Hanousek, F.; Štíbr, B.; Heřmánek, S. *Collect. Czech. Chem. Commun.* **1984**, *49*, 2776−2789.

(31) Wilkinson, F.; Helman, W. P.; Ross, A. B. *J. Phys. Chem. Ref. Data* **1995**, *24*, 663−1021.

(32) Ricchelli, F. *J. Photochem. Photobiol. B* **1995**, *29*, 109−118.

(33) DeCamp, D. L.; Babe, L. M.; Salto, R.; Lucich, J. L.; Koo, M. S.; Kahl, S. B.; Craik, C. S. *J. Med. Chem.* **1992**, *35*, 3426−3428.

(34) Miller, G. G.; Romanova, V. S.; Pokidysheva, L. N.; Totova, I. V.; Kaliberd, E. N.; Rumsh, L. D.; Andreeva, O. I.; Rybalkin, N. P. *Antibiot. Khimioter.* **2004**, *49*, 3−8.

(35) Dash, C.; Rao, M. *J. Biol. Chem.* **2001**, *276*, 2487−2493.

(36) Judd, D. A.; Nettles, J. H.; Nevins, N.; Snyder, J. P.; Liotta, D. C.; Tang, J.; Ermolieff, J.; Schinazi, R. F.; Hill, C. L. *J. Am. Chem. Soc.* **2001**, *123*, 886−897.

(37) Chen, S. X.; Wan, M.; Loh, B. N. *Planta Med.* **1996**, *62*, 381−382.

(38) Tyagi, S. C. *Biochem. Cell Biol.* **1992**, *70*, 309−315.